Received: 21 January 2022 | Revised: 23 May 2022 | Accepted: 27 June 2022

DOI: 10.1002/jex2.51

RESEARCH ARTICLE

Circulating extracellular vesicles provide valuable protein, but not DNA, biomarkers in metastatic breast cancer

Mercedes Tkach[1] | **Caroline Hego**[2] | **Marc Michel**[3] | **Lauren Darrigues**[4,5] | **Jean-Yves Pierga**[2,5,6] | **François-Clément Bidard**[2,6,7] | **Clotilde Théry**[1] | **Charlotte Proudhon**[3]

[1]Institut Curie, INSERM U932, PSL Research University, Paris, France

[2]Circulating Tumor Biomarkers laboratory, Institut Curie, INSERM CIC BT-1428, PSL Research University, Paris, France

[3]Institut Curie, INSERM U934/CNRS UMR3215, PSL Research University, Paris, France

[4]Department of Surgical Oncology, Institut Curie, Paris, France

[5]Université Paris-Cité, Paris, France

[6]Department of Medical Oncology, Institut Curie, Paris and Saint Cloud, France

[7]UVSQ, Université Paris-Saclay, Saint Cloud, France

Correspondence
Clotilde Théry, Institut Curie, INSERM U932, PSL Research University, Paris, France.
Email: clotilde.thery@curie.fr

Charlotte Proudhon, Institut Curie, INSERM U934/CNRS UMR3215, PSL Research University, Paris, France.
Email: charlotte.proudhon@inserm.fr

Clotilde Théry and Charlotte Proudhon have equal contribution and co-corresponding authorship.

Mercedes Tkach and Caroline Hego contributed equally.

Abstract

Detection of cell-free circulating tumour DNA (ctDNA) and cancer-specific extracellular vesicles (EVs) in patient blood have been widely explored as non-invasive biomarkers for cancer detection and disease follow up. However, most of the protocols used to isolate EVs co-isolate other components and the actual value of EV-associated markers remain unclear. To determine the optimal source of clinically-relevant circulating biomarkers in breast cancer, we applied a size exclusion chromatography (SEC) procedure to analyse separately the content in nucleic acids of EV-enriched and EV-depleted fractions, in comparison to total plasma. Both cellular and mitochondrial DNA (cellDNA and mtDNA) were detected in EV-rich and EV-poor fractions. Analysing specific mutations identified from tumour tissues, we detected tumour-specific cellular alleles in all SEC fractions. However, quantification of ctDNA from total plasma was more sensitive than from any SEC fractions. On the other hand, mtDNA was preferentially enriched in EV fractions from healthy donor, whereas cancer patients displayed more abundant mtDNA in total plasma, and equally distributed in all fractions. In contrast to nucleic acids, using a Multiplexed bead-based EV-analysis assay, we identified three surface proteins enriched in EVs from metastatic breast cancer plasma, suggesting that a small set of EV surface molecules could provide a disease signature. Our findings provide evidence that the detection of DNA within total circulating EVs does not add value as compared to the whole plasma, at least in the metastatic breast cancer patients used here. However, analysis of a subtype of EV-associated proteins may reliably identify cancer patients. These non-invasive biomarkers represent a promising tool for cancer diagnosis and real-time monitoring of treatment efficacy and these results will impact the development of therapeutic approaches using EVs as targets or biomarkers of cancer.

KEYWORDS

biomarkers, breast cancer, DNA, exosomes, extracellular vesicles, liquid biopsy, plasma, surface protein

1 | INTRODUCTION

Studying circulating extracellular vesicles (EVs) and their potential as non-invasive biomarkers in oncology has been the focus of intense research from both academic and pharmaceutical groups (Hoorn et al., 2005; Skog et al., 2008). EV-associated proteins, mRNA, miRNA, and even recently DNA have been explored as markers of disease progression, or response to therapy, especially in cancer, with few successes so far (Daly & O'Driscoll, 2021; Jia et al., 2017; Matsuzaki & Ochiya, 2017). Large tumour-derived extracellular vesicles (tdEVs) have been shown to have an equivalent prognostic power than circulating tumour cells (CTC) in castration-resistant prostate cancer (Nanou et al., 2018; Nanou et al., 2020). The same group demonstrated the possibility to detect HER2 at the surface of tdEVs with the same clinical significance than CTC in metastatic breast cancer patients (Nanou et al., 2020). This remains to be validated in prospective studies. Detection of a transmembrane glypican (Melo et al., 2015) or a combination of four transmembrane proteins and four miRNA in serum-derived EVs of pancreatic cancer (Madhavan et al., 2014), or of two cancer-specific mRNA in urine-derived EVs from prostate cancer patients (Donovan et al., 2015), have been proposed as reliable markers of advanced cancer but these results await confirmation by other groups. Detection of tumour-specific mutations in DNA associated with circulating EVs has also been proposed as a source of cancer biomarker (Kahlert et al., 2014; Lázaro-Ibáñez et al., 2014; Thakur et al., 2014). Interestingly, Lazaro-Ibanez observed different tumour-derived mutations in DNA associated to different EV subtypes. However, other studies proposed that total plasma DNA combined with mRNA present in EVs (Krug et al., 2017) or non EV-associated cell free DNA (Klump et al., 2018) are a better source than purified EVs to identify mutated DNA in lung cancer or melanoma and mastocytosis patients, respectively. Another study showed that circulating DNA in prostate cancer patients was recovered mainly either in large EVs, or in EV-depleted plasma, rather than in small EVs (Vagner et al., 2018). More recently, a study showed an equivalent sensitivity for mutation detection from EV-derived DNA and cell-free DNA in colon cancer (Thakur et al., 2021). The best source of tumour-derived DNAs in blood of patients is thus still unclear. We recently demonstrated that EVs or exosome preparations can contain co-isolated soluble proteins of serum or plasma origin, which can thus confound identification of EV-associated biomarkers in blood (Liao et al., 2019). In addition, it was recently demonstrated that other extracellular nanoparticles (ENP) called exomeres, are co-isolated with EVs and could contain part of some of the previously thought exosome- or EV-specific components (Jeppesen et al., 2019; Zhang et al., 2018). Methods to isolate EVs are thus critical for biomarkers analyses in order to decipher the various subtypes of EVs and various co-isolated components, which hold heterogenous compositions, functional activities and values as biomarkers. These observations have convinced us of the need to explore systematically the molecular content of EV and non-EV fractions of plasma, to pinpoint the best EV preparations to use in therapeutic or diagnostic applications.

To examine in which compartment DNA molecules are preferentially located and if enrichment of such compartment provides better sensitivity than analysing unprocessed total plasma, we studied a cohort of plasma samples collected from patients with metastatic hormono-dependent breast cancer, in which various EVs have been shown to be involved in the progression and formation of metastases (Lowry et al., 2015). We have successfully applied a size exclusion chromatography procedure to plasma samples from healthy donors and breast cancer patients to compare molecules associated to EV-enriched or -depleted fractions with molecules detected in total plasma. Our findings show that the detection of DNA within circulating EVs does not add value compared to whole plasma analysis, at least in the metastatic breast cancer patients used here. However, analysis of a subtype of EV-associated proteins may reliably identify cancer patients. These non-invasive biomarkers represent a promising tool for cancer diagnosis and real-time monitoring of treatment efficacy and our results will impact the development of therapeutic approaches using EVs as targets or biomarkers of cancer.

2 | MATERIALS AND METHODS

2.1 | Plasma samples

Blood samples from healthy donors were collected by the French blood establishment (agreement #16/EFS/031) under French and European ethical practices. Blood samples from women with estrogen receptor-positive (ER+) HER2-negative (HER2-) metastatic breast cancer (MBC) were collected, after written informed consent, in the frame of the ALCINA study (NCT02866149). Eligibility criteria were: patients aged ≥18 years with ER+, HER2- MBC, treated at Institut Curie (Paris and Saint Cloud, France) who progressed under endocrine therapy and for which a treatment with palbociclib and fulvestrant was being initiated. Tumour response to therapy was assessed at least every 3 months and classified, per RECIST v1.1 criteria, as complete response (CR), partial response (PR), stable disease (SD) or progressive disease (PD). For each patient, samples were collected at the time of inclusion before the start of the treatment.

All samples from patients and healthy donors were collected in EDTA tubes and plasma was isolated within 4 h to ensure a good quality of circulating cell-free DNA (cfDNA). Blood samples were centrifuged at 820 g for 10 min, followed by a second centrifugation at 16,000 g for 10 min (Table S1) and plasma was stored at −80°C until use.

2.2 | Size Exclusion Chromatography (SEC)-based separation of EVs from plasma

EVs were isolated from 2 ml of plasma using SEC (qEV original 70 nm/Izon). Elution fractions of 0.5 ml were collected. Based on the Nanoparticle Tracking and Western blot analyses, we further defined three pools of elution fractions: (1) EV-enriched pools (F7-11), (2) intermediate pools (F12-17), and (3) EV-poor pools (F18-24).

2.3 | Western blot and NTA

Western blots (WB) and Nanoparticle tracking analyses (NTA) were performed on ultracentrifugation (UC) pellets (30′ at 100,000 g, TLA-45 rotor) of each SEC elution fraction obtained from 2 ml of healthy plasma, isolated as described above. Pellets were resuspended in 15 μl of PBS, 13 μl were used for WB, and 2 μl for NTA. NTA was performed using ParticleMetrix ZetaView PMX-20 with software version 8.04.02. The instrument settings were sensitivity of 75 and shutter of 75. Measurements were done at 11 different positions (five cycles per position) and a frame rate of 30 frames per second.

WB were performed using Laemmli sample buffer without reducing agent (BioRad). After boiling 5 min at 95°C, samples were loaded on a 4–15% Mini-protean TGX-stain free gels (BioRad). Transfer was performed on Immuno-Blot PVDF membranes (BioRad), with the Trans-blot turbo transfer system (BioRad) during 7 min. Blocking was performed during 30 min with Roche blotting solution in TBS 0.1% Tween. Primary antibodies were incubated overnight at 4°C and secondary antibodies (HRP-conjugated goat anti-rabbit IgG (H + L), goat anti-mouse IgG (H + L), goat anti-chicken IgY IgG (H + L) and goat anti-rat IgG (H + L), Jackson Immuno-Research) during 1h at room temperature (RT). Development was performed using Clarity western ECL substrate (BioRad) and the Chemidoc Touch imager (BioRad). Antibodies were: mouse anti-human CD63 (clone H5C6, BD Bioscience), mouse anti-human CD9 (clone MM2/57, Millipore), mouse anti-human MHCI HLA-ABC (W6/32, ThermoFisher), chicken anti-ApoA1 (#GTX8515, Genetex). Monoclonal rabbit anti-human syntenin was a gift from P. Zimmermann (CRC Marseille France, and Univ Leuven, Belgium).

2.4 | DNA isolation and quantification

cfDNA was isolated from SEC fraction pools using the Qiamp Circulating Nucleic Acid kit (Qiagen) according to the manufacturer's protocol. For each patient or healthy sample, we also isolated cfDNA from 1 to 4 ml of total plasma that did not undergo SEC, using the same procedure, except for 17 breast cancer samples that were isolated with QIAsymphony DSP circulating kit (Qiagen) according to the manufacturer's protocol (this is detailed in Table S1). We have compared the DNA yield efficiency of total plasma extracted with the two methods and did not observe any differences (Figure S1a-c). cfDNA concentrations were measured using the High Sensitivity dsDNA Qubit Assay, which is based on a DNA-selective dye that emits fluorescence measured with the Qubit 2.0 fluorometer (Thermo Fisher). Amplifiable cellular cfDNA (cellDNA) was quantified using a quantitative PCR (qPCR) assay targeting LINE1 elements. PCR was performed in a 25 μl total volume with the following components: 20 μM of forward primer (5′AGGGACATGGATGAAATTGG3′), 20 μM of reverse primer (5′ TGAGAATATGCGGTGTTTGG3′), 12.5 μl of 2X Power SYBR Green PCR Master Mix (Thermofisher), 10 μl of molecular biology grade water and 2 μl of DNA input. A serial dilution of normal human peripheral blood mononuclear cells (PBMC) DNA was incorporated in each plate as a standard. All real-time PCR assays were carried out in a 7900 Fast real-time PCR system (Thermofisher). The reaction was monitored with the following cycling conditions: One cycle at 95°C for 5 min, followed by two cycles of (95°C for 10 s, 67°C for 15 s and, 72°C for 15 s), two cycles of (95°C for 10 s, 64°C for 15 s and, 72°C for 15 s), two cycles of (95°C for 10 s, 61°C for 15 s and, 72°C for 15 s), 30 cycles of (95°C for 10 s, 59°C for 15 s and, 72°C for 33 s), and a final cycle of (95°C for 15 s, 60°C for 1 min and, 95°C for 15 s). The baseline and the cycle threshold value (Ct) were set using the Thermofisher software.

Amount of mitochondrial DNA (mtDNA) was determined by qPCR for the human ND5 gene using primers from Sansone and colleagues (Sansone et al., 2017). To prepare a 25 μl PCR reaction, we used 2X of Power SYBR Green PCR Master Mix (Thermofisher), 20 μM of forward primer (5′TTACCACCCTCGTTAACCCTAACAAA3′) and 20 μM of reverse primer (5′TGGGTTGTTTGGGTTGTGGCT3′), 10 μl of molecular biology grade water and 2 μl of DNA input. A serial dilution of total genomic DNA (including cellDNA and mtDNA), isolated from the MCF7 breast cancer cell line was incorporated in each plate as a standard. DNA was amplified with a Quantstudio 5 Real-time PCR system (Thermofisher) with the following program: One cycle at 95°C for 10 min, 35 cycles at 95°C for 15 s, 47°C for 15 s and 72°C for 30 s. Results were analysed with the QuantStudio 3 and 5 Real-Time PCR System Software (Thermofisher).

2.5 | Tumour DNA quantification by droplet digital PCR

Mutations in primary tumours of each patient were previously characterized by NGS (Darrigues et al., 2021; Jeannot et al., 2020). Droplet digital PCR (ddPCR) using assays targeting specific mutations (Table S3) identified by NGS were performed

on cfDNA with the following conditions: 20 μL final volume, including 10 μl of ddPCR Supermix for probes (No dUTP, Bio-Rad), 900 nM/250 nM of each primer/probe respectively, 5 μl of water and 5 μl of DNA. The mixture was transferred to DG8 cartridge for ddPCR (Biorad) with 70 μl of Droplet Generation Oil. Droplet generation was performed using the Bio-Rad droplet generator (QX100). The droplets were transferred to a 96-well plate (Bio-Rad) and loaded into the C1000 Touch thermocycler (Bio-Rad) for PCR amplification according to the following parameters: One cycle at 95°C for 10 min, followed by 40 cycles at (94°C for 30 s, 60°C for 1 min for PIK3CA mutations or 55°C for the other mutations) and a final cycle at 98°C for 10 min. Droplet fluorescence was measured using QX100 droplet reader and the results were analysed with Quantasoft software (Biorad).

2.6 | HCT116 tumour DNA spiked-in

To validate the tumour DNA quantification assay on SEC fractions of plasma, we used serum-free medium (ATCC-formulated McCoy's 5A medium modified) conditioned for 24h by 40.10^6 HCT116 cells (colorectal carcinoma cell line) and concentrated to 300 μl by filter-centrifugation on 100 kDa ultrafiltration units (Merck Millipore). We spiked 100 μl of this EV-containing concentrated conditioned medium (CCM) in 2 ml of healthy donor plasma (previously centrifuged at 820 g and 16,000 g) before SEC separation and DNA extraction. We then checked if the mutation of interest was detected by ddPCR in plasma.

2.7 | Statistical analyses

Friedman tests were used to compare total DNA (Qubit), cellular DNA (cellDNA, LINE-1) and mitochondrial DNA (mtDNA, ND5) in the various fractions of healthy or breast cancer plasma to allow multiple comparisons between the four fractions. Mann-Whitney t-tests were used to compare the same fractions of healthy and breast cancer plasma of total DNA, cellDNA or mtDNA. Welch's t-tests were used to compare the number of copies (Mut, WT and total) per ml of plasma and the mutant allele frequencies in each plasma fractions of breast cancer patients. Kruskal-Wallis tests were used to compare healthy versus breast cancer plasma from patients with different tumour burden or disease progression status (See Table S2 for more details). Differences between fluorescence intensities of EV surface markers in healthy donors and breast cancer plasma were studied using Mann–Whitney U tests.

2.8 | EV surface protein analysis

We set up a multiplexed analysis of 37 EV surface proteins from EV-enriched SEC fractions, using the MACSPlexExo kit, human (Myltenyi (Koliha et al., 2016)). Samples were processed according to manufacturer instructions. 1.5 ml plasma biobanked at −80°C after 820 g and 16,000 g centrifugation (as described in section "plasma" above), was thawed up at room temperature before loading on qEV70 "original" (Izon, designed for 0.5 ml samples). Fractions of 0.5 ml were collected and EV-enriched fractions 7–11 were further concentrated by ultracentrifugation for 30′ at 100,000 g in a TLA 110 rotor (Beckman, Optima TL100 centrifuge) and pellets resuspended in 20 μl PBS were diluted with MACSPlex buffer to a final volume of 120 μL and distributed in the MACSPlex Filter plate. 15 μL of MACSPlex Exosome Capture Beads were added. Samples were incubated on an orbital shaker overnight at room temperature protected from light. After washing twice with the MACSPlex buffer, 5 μl of each detection antibody were added (APC conjugated anti-CD9, anti-CD63, and anti-CD81) and samples were incubated for 1h at RT. Samples were washed with 200 μl of MACSPlex Buffer. Flow cytometric analysis was performed with a Cytek Aurora with the following configuration: FSC Threshold 50000, APC Detector Voltage 1100, FITC Detector Voltage 60, PE Detector Voltage 60). FlowJo software (v10, FlowJo LLC) was used to analyse flow cytometric data. The 39 single bead populations were gated to allow the determination of the APC signal intensity on the respective bead population. Median fluorescence intensity (MFI) for each capture bead was background corrected by dividing respective MFI values with matched non-EV controls that were treated exactly like EV-containing samples. For capture antibodies for which the corresponding isotype control (mIgG1 or REA) was provided in the kit, a second normalization was performed for each sample, by dividing the normalized MFI of the capture bead by normalized MFI of the isotype control. Capture beads coated with mIgG2 antibodies that could not be analysed this way were: CD1c, CD2, CD3, CD4, CD8, CD11c, CD14, CD49e, CD45. Values were log10 transformed. Only normalized log10 values higher than 0 were considered as positive.

2.9 | Breast cancer classifier based on the 'outlier' analysis

For each marker and each breast cancer patient, a distribution was created composed by all the healthy donors' samples together with the patient's sample. For each of these distributions, an outliers detection analysis was performed using the R package

'extremevalues' (van der Loo, 2010) as follows: the distributions were fitted to a theoretical exponential one, deemed closest to our data points distribution, and the function getOutliersI was used with default parameters (rho = c(1, 1), FLim = c(0.1, 0.9), distribution = "exponential") to detect potential outliers. Samples thus flagged as outliers were then translated to true positives (patients' samples) and false positives (healthy donors' samples). Only results originating from distributions fitting with an $R^2 \geq 0.7$ were used, to ensure statistically significant outlier detection.

3 | RESULTS

3.1 | Cell free genomic DNA is less abundant in EV-associated fractions than in total plasma

We wanted to determine if DNA molecules circulating in plasma were preferentially found in EV-rich fractions, and if selective analysis of EV-associated ctDNA provided better sensitivity or specificity than analysis of unprocessed total plasma. We, thus, implemented a size exclusion chromatography (SEC), which we had used before, to separate EVs from non-EV components in serum-containing culture medium (Liao et al., 2019). We tested the efficacy of this technique on plasma from healthy donors centrifuged at 16,000 g, following the standard plasma isolation procedure for cfDNA analysis (Riva et al., 2017). This second centrifugation is important to eliminate platelets and other cell-derived microparticles (Figure 1a). We counted the number of particles in each individual SEC fractions by Nanoparticle Tracking Analysis (NTA), which detects particles larger than 60 nm in diameter, and found three groups of fractions highly enriched in particles: F9, F13-15 and F20 (Figure 1b). Protein composition of the SEC fractions was analysed by Western blot using antibodies detecting EV-associated transmembrane proteins (CD63, CD9 and MHCI), an EV-enclosed soluble cytosolic protein marker (Syntenin), a high-density lipoprotein (HDL) marker (ApoA1) which should not be present in EVs, and total proteins (Figure 1c). EV-associated markers were found mainly in F8-11, whereas a majority of proteins and ApoA1 were recovered in F18-24. This led us to define three pools of SEC fractions corresponding to (i) EV-enriched and protein-poor fractions (F7-11: EV fractions), (ii) protein-rich and EV-poor fractions (F18-24: soluble fractions, which also contain HDL) and (iii) an intermediate pool containing a mixture of EVs and soluble proteins (F12-17: intermediate fractions) (Figure 1c). Downstream DNA analyses were performed on each pool of SEC elution fractions in parallel, and compared to unfractionated total plasma from the same subjects (Figure 1a). We first compared the amount of total circulating cell-free DNA (cfDNA) extracted from 15 healthy donors and 27 patients with hormone-dependent metastatic breast cancer by Qubit fluorometer quantification (Figure 1d; Table S1). We observed similar levels of cfDNA in EV fractions of healthy donors and cancer patients. In contrast, we detected more cfDNA in the intermediate and soluble fraction pools as well as in total plasma of several breast cancer samples compared to healthy donors (Figure 1d; Table S2). In these breast cancer patients specifically, we observed a higher cfDNA content in the intermediate fractions, soluble fractions and total plasma than in the EV-enriched pool. Two healthy donors displayed slightly higher levels of DNA than the average in total plasma, and one in EV fractions. We further quantified the amount of amplifiable cellular DNA (cellDNA) using a qPCR assay targeting LINE1 elements. In healthy donors, we could show that cellDNA is depleted from EV-enriched fractions compared to EV-poor fractions (F12-17 and F18-24). In turn, cellDNA content is lower in EV-enriched fractions than in total plasma (Figure 1e; Table S2). We observed the same trend in plasma from breast cancer patients, with less cellDNA detected in SEC fraction pools compared to unprocessed plasma, especially in the EV-associated pool ($P < 0.0001$ ****, Table S2). However, we also observed that there is statistically more cellDNA in all fractions of breast cancer plasma as compared to healthy donors ($P < 0.0001$ **** for all four fractions, Figure 1e; Table S2). Overall, DNA content (total cfDNA or amplifiable cellDNA) detected in the EV-enriched fractions was lower than in EV-depleted fractions or unprocessed plasma. This shows that the higher levels of circulating cfDNA previously described in patients suffering from advanced cancer (Chen et al., 2021; Stroun et al., 1987) is not primarily associated to EVs in plasma.

3.2 | Quantification of circulating tumour DNA from unprocessed plasma is more sensitive than from EV-enriched fractions

Even if total cfDNA and amplifiable cellDNA were not particularly abundant in circulating EVs, abnormal physiology of cancer cells could lead to specific enrichment of tumour-derived DNA in EVs. Therefore, we assessed if tumour alleles were enriched in EV-associated fractions. To validate the procedure for detecting tumour DNA from the different SEC fractions, we introduced tumour DNA from HCT116 cells, which carry a *PIK3CA* H1047R mutation, into healthy plasma. To do so, we spiked healthy plasma with concentrated conditioned medium (CCM) collected from HCT116 cells in culture and processed the reconstituted plasma by SEC. Tumour DNA copies were quantified with a droplet digital PCR (ddPCR) assay designed to identify the *PIK3CA* H1047R mutation. As expected, we specifically detected *PIK3CA* H1047R mutant copies when HCT116 CCM was added, whereas only WT copies were detected in plain healthy donor plasma (Figure 2a). We observed the same mutant allele fraction (MAF) in all SEC fraction pools and total plasma. This illustrates that spike-in from CCM, which includes EVs but also cell free DNA from the cell medium, leads to a homogeneous distribution of mutant DNA in the various SEC fractions.

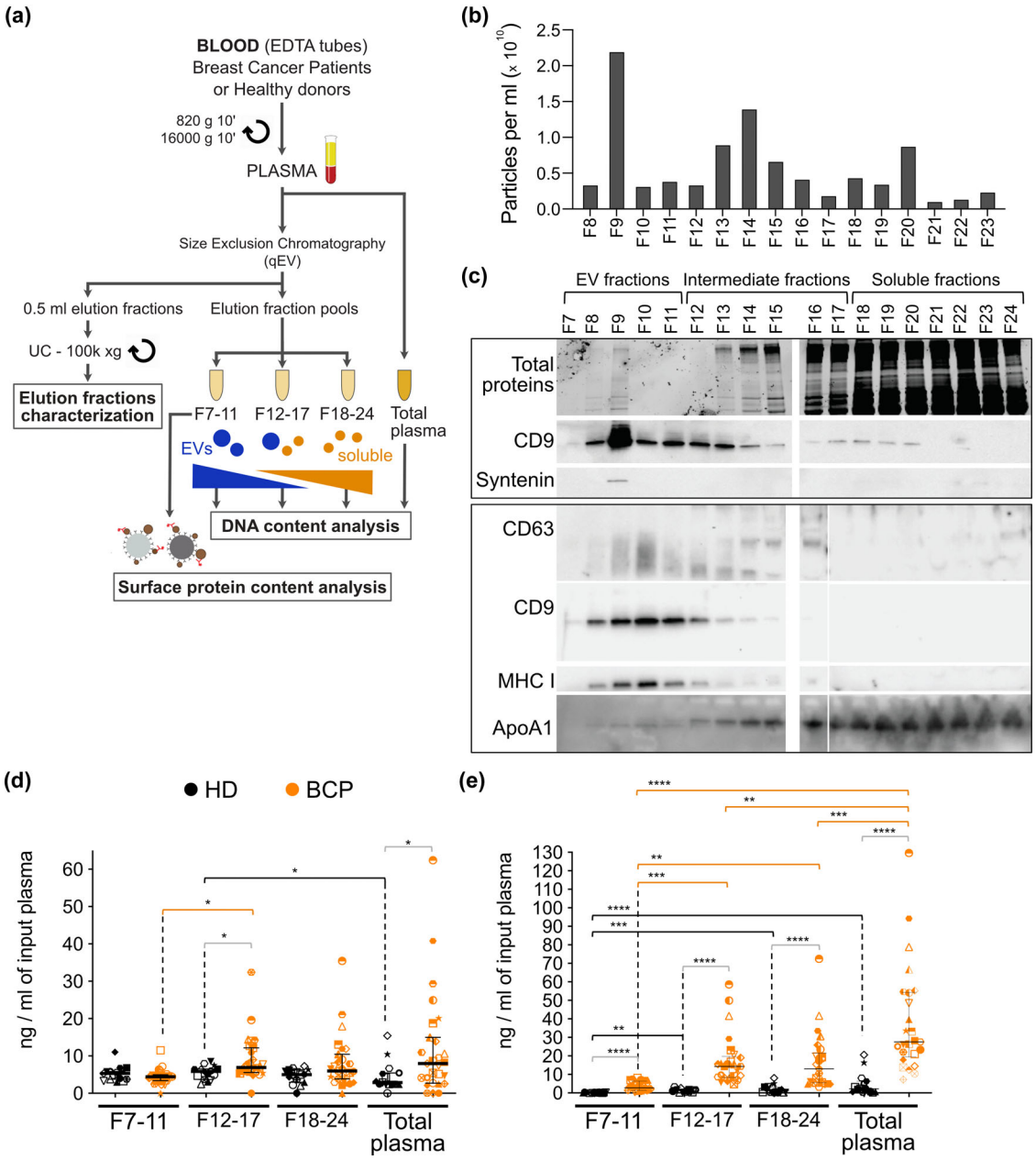

FIGURE 1 **Cell free genomic DNA is less abundant in EV-associated fractions than in total plasma.** (**a**). Experimental workflow to separate by Size-Exclusion Chromatography (SEC) EVs from smaller circulating components in plasma. Western blots (**c**) and Nanoparticle tracking analyses (**b**) were performed on ultracentrifugation (UC) pellets to characterize each elution fraction. Downstream DNA analyses (Figure 1**d-e,** Figure 2 and 3) were performed on each pool of fractions (EV-enriched fractions (F7-11), intermediate fractions (F12-17), soluble fractions (F18-24)) and total plasma in parallel. Surface protein analyses (Figure 4) were performed on EV-enriched fractions. (**b**). Particle count in each SEC fraction by nanoparticle tracking analysis. One representative experiment. (**c**). Protein composition analysis by Western blotting of all SEC fractions showing total proteins, EV-associated markers (three surface proteins: CD63, CD9 and MHCI, and one soluble cytosolic protein: Syntenin), and an EV-excluded protein (ApoA1). Top and bottom panels are from two independent experiments, CD9 distribution is shown in both to allow comparison. (**d-e**). Quantification of total DNA by fluorometric quantitation using Qubit (**d**) or amplifiable cellular DNA (cellDNA) using a LINE1 qPCR (**e**) in EV-enriched (F7-11), intermediate (F12-17) and soluble (F18-24) fractions versus total plasma in both healthy donors (HD, $N = 15$, black symbols) and breast cancer patients (BCP, $N = 27$, orange symbols). Thick black lines show the median with interquartile range. Orange bars highlight differences among BCP, black bars among HD and grey bars between BCP and HD. Only significant P-values are indicated, see Table S2 for more details on statistical results

We then quantified the amount of circulating tumour DNA (ctDNA) detected in the three pools of SEC fractions isolated from plasma of breast cancer patients ($N = 27$). Here, we targeted known mutations carried by each patient previously identified from their tumour ((Darrigues et al., 2021; Jeannot et al., 2020), Table S1), using specific ddPCR assays for these mutations (Table S3; Figure 2b). We detected more copies (WT, mutant or both taken together) in unprocessed plasma than in any SEC fraction pools (Figure 2c; Table S1). In comparison to EV-enriched fractions, the number of copies detected in unprocessed

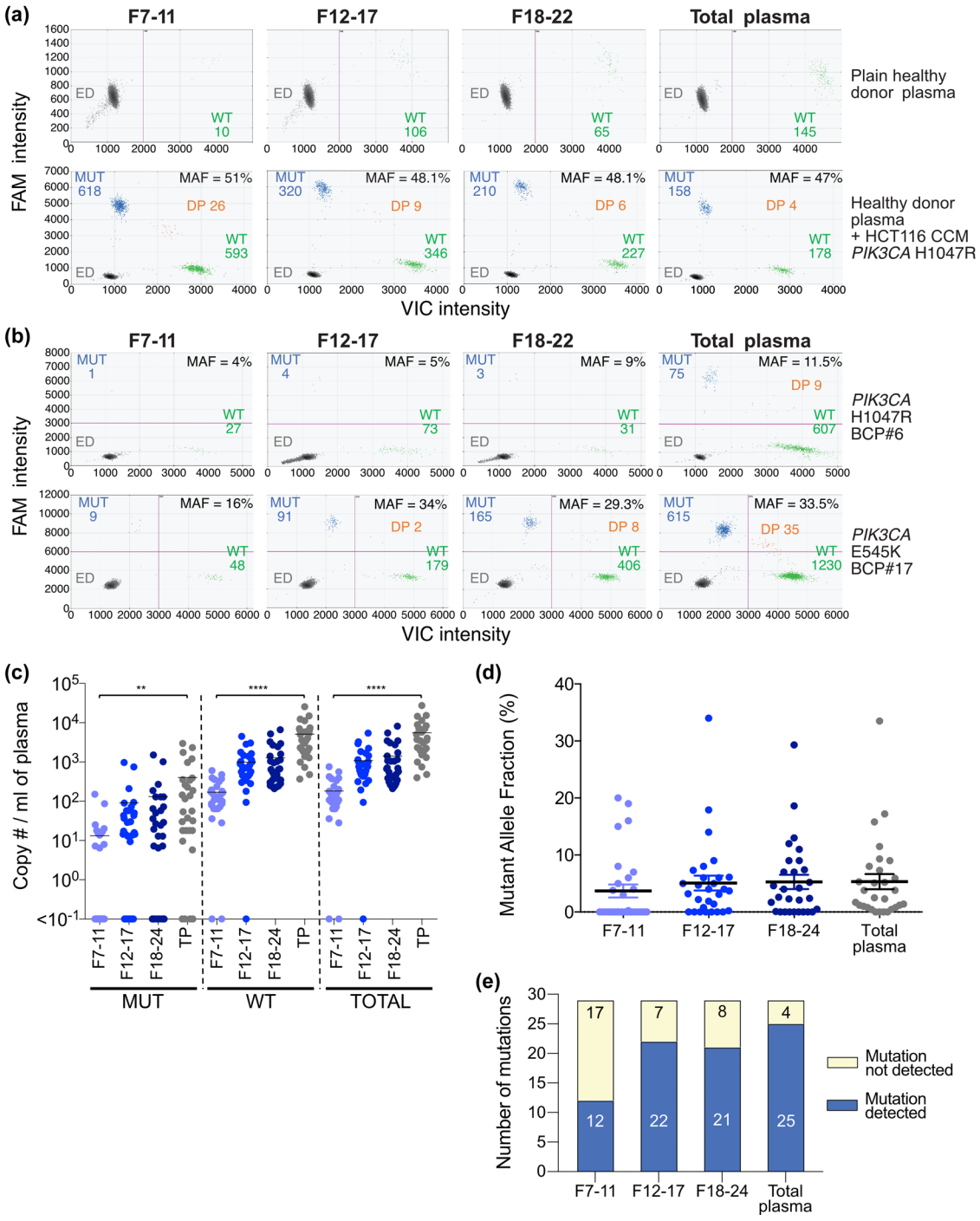

FIGURE 2 **Quantification of circulating** tumour **DNA from unprocessed plasma is more sensitive than from EV-enriched fractions.** (**a**). Tumour DNA detection in plasma SEC fractions through *PIK3CA* H1047R mutation analysis by ddPCR. We analysed plain healthy donor plasma (upper panels) or healthy plasma spiked with concentrated conditioned media (CCM) collected from HCT116 tumour cells (lower panels). MAF: mutant allele fraction, DP: double positive droplets (WT + PIK3CA MUT), ED: empty droplets. (**b**). *PIK3CA* mutation detection by ddPCR in plasma SEC fractions from breast cancer patients. Examples from two different patients with *PIK3CA* H1047R (P#6) or E545K (P#17) mutations. MAF = mutant allele fraction, DP: double positive droplets (WT + PIK3CA MUT), ED: empty droplets. (**c**). Number of mutant (MUT), wild-type (WT) or total copies detected by ddPCR in each elution fraction pools and total plasma (TP) of breast cancer patients ($N_{Patients} = 27$, $N_{Mutations} = 29$). $p_{MUT} = 0.009$, $p_{WT} < 0.0001$, $p_{TOT} < 0.0001$. (**d**). Mutant allele fractions (MAF) in each SEC elution pool and total plasma (TP) of breast cancer patients ($N_{Patients} = 27$, $N_{Mutations} = 29$). Black lines display the means, color lines SD. The number of samples with MAF = 0% correspond to the samples with no mutations detected in (**e**). (**e**). Number of known mutations detected versus not detected in each SEC fraction pool and total plasma of breast cancer patients ($N_{Patients} = 27$, $N_{Mutations} = 29$). The mutations targeted were previously identified from each patient's tumour tissues (see Table S1)

total plasma was statistically significantly higher (Figure 2c; $p_{MUT} = 0.009$, $p_{WT} < 0.0001$, $p_{TOT} < 0.0001$). Additionally, we observed that the sum of the number of copies detected in the three elution fraction pools was lower than the number of copies detected in total plasma (Figure S1d). This demonstrates that separation of plasma fractions may result in material loss during the procedure. Even if the average percentage of mutant alleles did not statistically vary between plasma fractions (Figure 2d), we observed a greater sensitivity for mutation detection from unprocessed plasma samples (Figure 2e). Moreover, mutation detection from soluble fractions was more sensitive than from EV-enriched fractions. This indicates that EV fractions are not particularly enriched in tumour DNA and clearly highlights that processing plasma to isolate SEC fractions leads to loss of material and does not improve the detection of tumour copies. Overall, in our cohort of breast cancer patients, quantification of tumour DNA from total unfractionated plasma shows better sensitivity than quantification from EV-enriched SEC fractions.

3.3 | Isolation of plasma EVs does not improve the quantification of mitochondrial DNA (mtDNA) for disease detection or monitoring

Mitochondrial DNA (mtDNA) has been shown to be present in EVs recovered by ultracentrifugation and density gradient from plasma of therapy-resistant breast cancer patients with similar clinical features to those of our cohort (Sansone et al., 2017). Using a qPCR assay targeting the mitochondrial gene ND5, we quantified mtDNA in EV-rich and EV-poor SEC fractions in comparison to total plasma from the same breast cancer patients and healthy donors. MtDNA quantification from the total plasmas of six patients came back inconclusive and the complete data of these patients were eliminated for this analysis ($N_{BCP} = 21$, $N_{HD} = 15$). We observed a significant higher abundance of mtDNA in the EV-containing fractions (F7-11) and the total plasma of healthy donors compared to their EV-poor fractions (F18-24) (Figure 3a; Table S2; $p_{HD(F7\text{-}11vsF18\text{-}24)} < 0.0001$, $p_{HD(F18\text{-}24vsTP)} = 0.0005$). In breast cancer patients, we only observed a significant higher abundance of mtDNA in the total plasma compared to the EV-poor fractions (F12-17 and F18-24) (Figure 3a; Table S2; $p_{BCP(F12\text{-}18vsTP)} = 0.036$, $p_{BCP(F18\text{-}24vsTP)} < 0.0001$). Indeed, in healthy donors, we consistently observed a lower level of mtDNA in EV-poor fraction F18-24, whereas the levels detected in EV-rich fractions F7-11 were similar to the levels detected in total plasma. (Figure 3b). In breast cancer patients we observed an enrichment of mtDNA specifically in total plasma (Figure 3c). We also observed higher quantities of mtDNA in breast cancer patients as compared to healthy donors in each fraction, with a statistical difference in total plasma and its soluble fraction F18-24 (Figure 3a; Table S2; $p_{Total\ Plasma} = 0.0003$, $p_{F18\text{-}24} = 0.0049$). This illustrates that the higher levels of mtDNA released to the circulation in breast cancer patients is not necessarily associated to EVs, and may also be associated to other components that can be separated from EVs by SEC. Overall, circulating mtDNA displays a different distribution than cellDNA and is more likely recovered from EVs than other carriers in healthy plasma, but not in breast cancer patients.

We further analysed if the levels of mtDNA correlated with the disease burden or were predictive of the response to treatment. First, patients were classed in two groups relative to their number of metastatic sites. We defined a group with low disease burden with two or less metastatic sites and a group with high disease burden with more than two metastatic sites (Figure S2). We observed a trend for mtDNA enrichment in cancer patients with high disease burden, with significant differences in total plasma and its soluble fraction F18-24 as compared to healthy donors. Total plasma of patients with low disease burden also displayed significantly higher level of mtDNA than those of healthy donors, and there was no statistical differences between patients with low and high disease burden (Figure 3d; Table S2; $p_{F18\text{-}24(HD\ vs\ BCP\ high\ DB)} = 0.0308$, $p_{Total\ plasma(HD\ vs\ BCP\ low\ DB)} = 0.0214$, $p_{Total\ plasma(HD\ vs\ BCP\ high\ DB)} = 0.0039$). The disease progression status was determined after 3-month of treatment by clinical evaluation based on RECIST v1.1 criteria. We divided patients in two groups with progressive disease (PD) versus non-progressive disease (non-PD). We observed a statistically different enrichment for mtDNA in total plasma for both PD and non-PD patients and only in patients with non-PD in soluble fractions F18-24 as compared to healthy donors but there was no statistical differences between patients with progressive and non-progressive disease (Figure 3e; Table S2; $p_{F18\text{-}24(HD\ vs\ BCP\ non\text{-}PD)} = 0.0044$, $p_{Total\ plasma(HD\ vs\ BCP\ non\text{-}PD)} = 0.0012$, $p_{Total\ plasma(HD\ vs\ BCP\ PD)} = 0.0459$). Overall, we observed more mtDNA in the total plasma of both subgroups of patients but there were no significant differences between the subgroups, relative to the disease burden or the disease progression. Therefore, analysing mtDNA in total plasma or specific fractions, including isolated EVs, did not provide any useful prognostic or diagnostic information on the patient's status. This illustrates that isolation of EVs does not improve the quantification of cancer-related DNA for disease detection or monitoring, at least in the metastatic breast cancer patients used here.

3.4 | A subset of EV surface proteins reliably identify breast cancer patients

Since the DNA content associated to plasma EVs does not represent a useful biomarker in our cohort of breast cancer patients, we analysed the EV-associated protein components, looking for more specific biomarkers. We examined the distribution of plasma EV surface proteins in nine breast cancer patients versus nine healthy donors, using a commercial EV capture test which allows

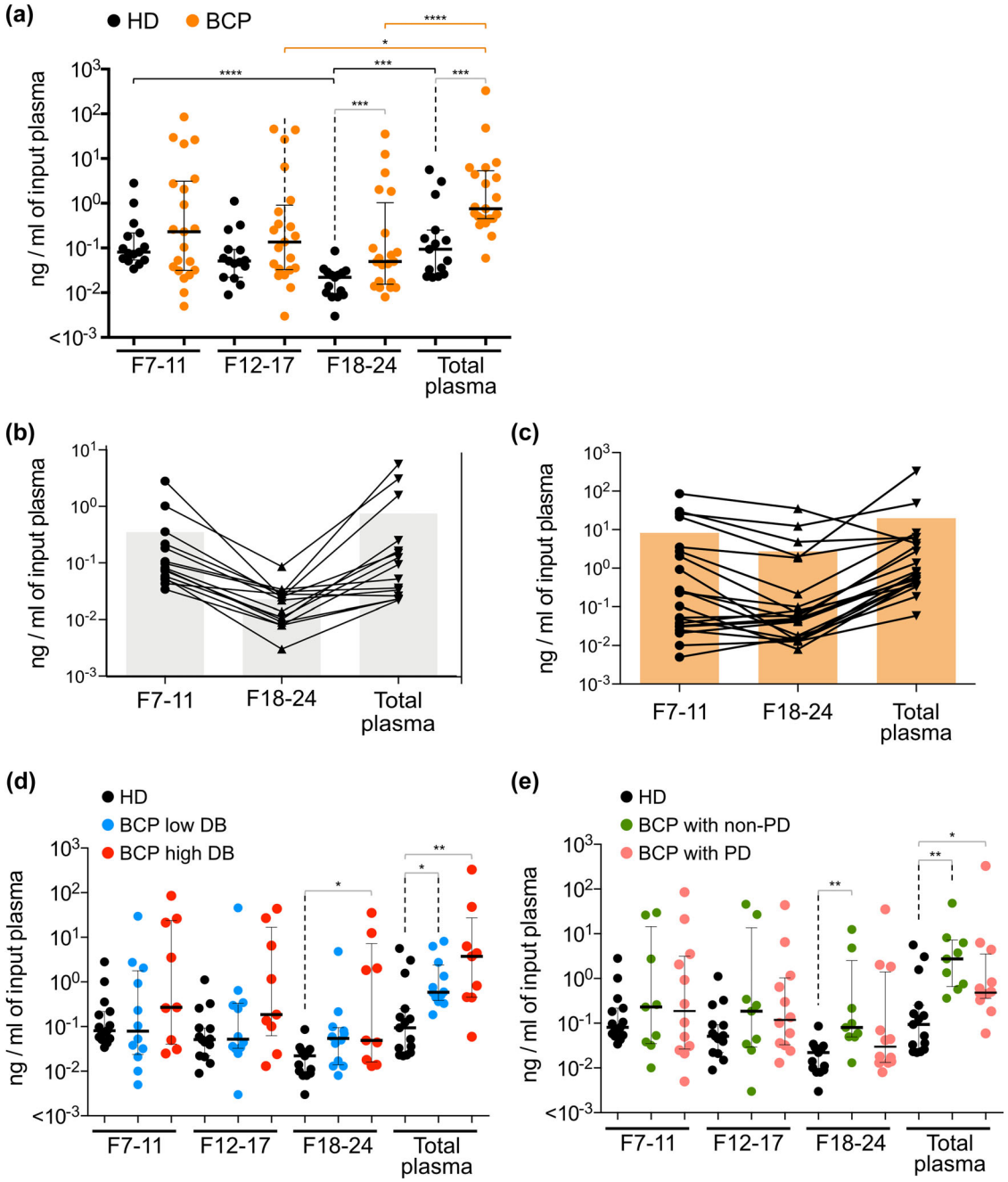

FIGURE 3 **Isolation of plasma EVs does not improve the quantification of mitochondrial DNA (mtDNA) for disease detection or monitoring. (a)**. Amount of mitochondrial DNA (mtDNA), quantified by quantitative PCR targeting the ND5 gene, in SEC fractions and total plasma of healthy donors (HD, $N = 15$, black circles) and breast cancer patients (BCP, $N = 21$, orange circles). Thick black lines show the median with interquartile range. Only significant *P*-values are indicated, see Table S2 for more details on statistical results. **(b-c)**. Donor-specific comparisons of mtDNA levels detected in EV-enriched, EV-depleted and total plasma of each healthy donor (b) or breast cancer patient (c). This is another representation of the data displayed in 3A. **(d)**. Amount of mtDNA in SEC fractions of healthy donors as compared to patients classified by disease burden (DB): high (> 2 metastatic sites) or low (≤2 metastatic sites). Only significant *P*-values are indicated, see Table S2 for more details on statistical results. **(e)**. Amount of mtDNA in SEC fractions of healthy donors as compared to patients displaying progressive disease (PD) or not (non-PD). Only significant *P*-values are indicated, see Table S2 for more details on statistical results

analysis, by flow cytometry, of the presence of 37 membrane-exposed protein markers on EVs which also bear CD9, CD63, and/or CD81, transmembrane tetraspanins classically used as markers of small EVs (Koliha et al., 2016). We used the total EVs recovered from F7-11 SEC fractions of plasma stored at -80°C as it is had been done for ctDNA isolation. We first counted the number of particles by Nanoparticle Tracking Analysis (NTA) and found a significantly increased number of EVs in the plasma of breast cancer patients (Figure S3a). This was correlated with a generally higher level of raw MFI values for most analysed markers in the

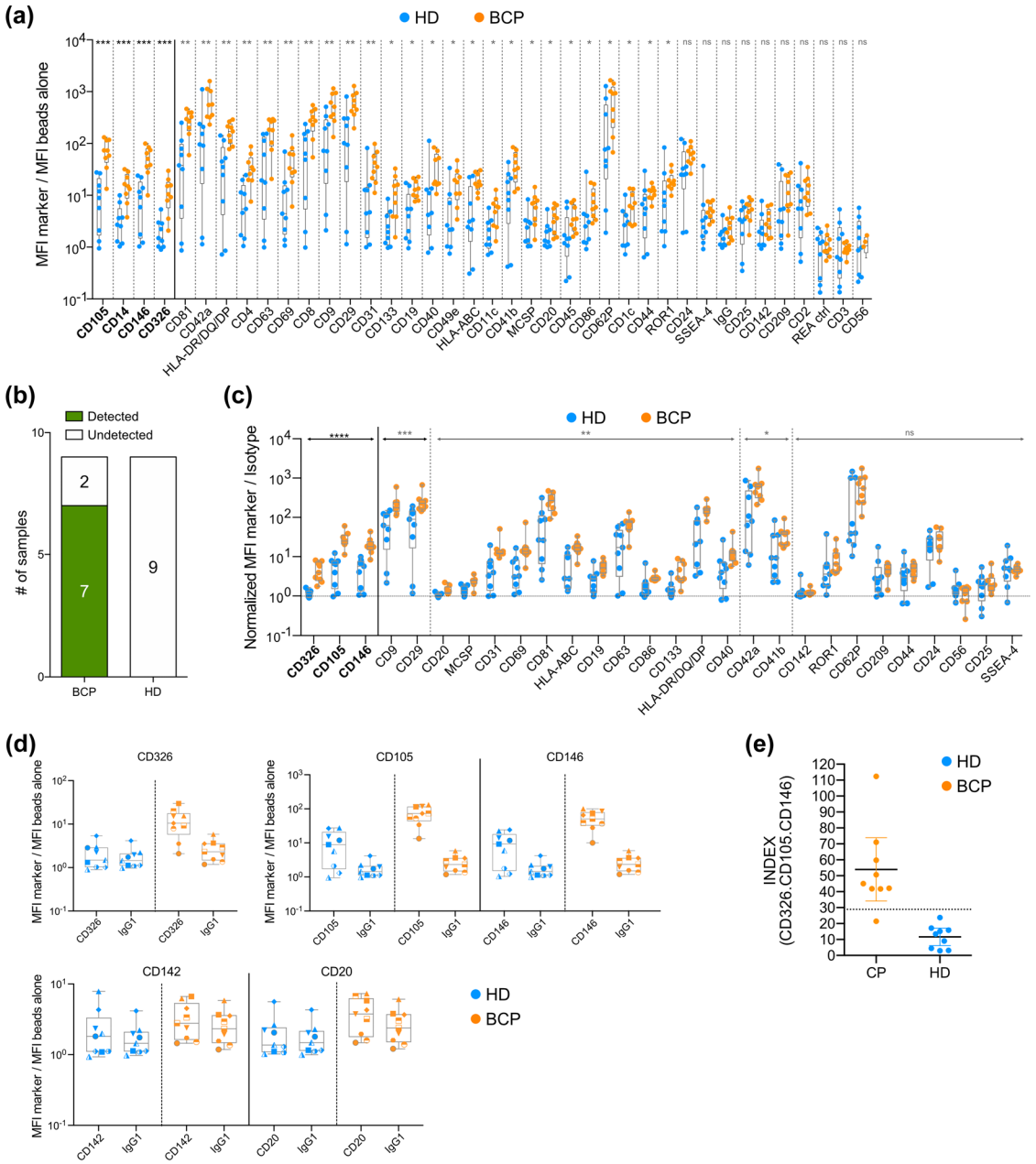

FIGURE 4 **A subset of EV surface proteins reliably identify breast cancer patients. (a)**. Distribution of the mean fluorescence intensity (MFI), normalized by the MFI of beads alone, for each of the 37 membrane protein markers and two isotype controls, Recombinant Antibody (REA) and mIgG1, in breast cancer patients ($n = 9$) versus healthy donors ($n = 9$). The markers are ordered by differential distribution significance (Mann–Whitney U test P-values). The four markers the most significantly enriched in breast cancer patients are highlighted in bold. **(b)**. Number of samples detected as breast cancer patients using our 4-surface-marker classifier. (**c**). Ratios of the normalized MFI of each marker over their isotype controls. Only markers for which the corresponding control isotype was included in the analysis (mIgG1 and REA) are displayed. The three markers the most significantly enriched in breast cancer patients are highlighted in bold. **(d)**. Normalized MFI of the three markers the most significantly enriched in breast cancer patients versus two markers either less significantly enriched (CD20), or non-significantly different (CD142), compared to the normalized MFI of the isotype control beads. (**e**). Distribution of arbitrary indexes calculated by summing the three ratios of the normalized MFI of CD326, CD105 and CD146 for BCP versus HD. The dashed line marks the computed threshold (HD Index mean + 95% CI = 28.86)

patient's as compared to the healthy donor's samples (Figure S3b). Next, we analysed the data by calculating, for each antibody-coated bead, its median fluorescence intensity (MFI) in the presence of EVs divided by its background MFI in the absence of EVs (Figure 4a). We observed that four proteins, CD326 (gene *EPCAM*), CD146 (= MUC18, gene *MCAM*), CD105 (= endoglin, gene *ENG*) and the monocyte differentiation antigen CD14, were highly significantly enriched ($P < 0.001$) in breast cancer patients EVs compared to healthy donors (Figure 4a). We further developed a pipeline to automatically call markers with statistically different distribution in patients as compared to healthy donors (R package 'extremevalues' for the detection of outliers – see

TABLE 1 Outlier classification for the four most significantly different markers (P-values < 0.001)

		Outlier classification - markers with P-values < 0.001								
Patient	**Marker**	**P#24**	**P#22**	**P#23**	**P#21**	**P#31**	**P#25**	**P#14**	**P#30**	**P#27**
#24	**CD14**	FALSE	TRUE	TRUE	TRUE	TRUE	FALSE	FALSE	TRUE	TRUE
	CD105	FALSE	TRUE	TRUE	TRUE	TRUE	FALSE	TRUE	TRUE	TRUE
	CD146	FALSE	TRUE	TRUE	TRUE	TRUE	FALSE	TRUE	TRUE	TRUE
	CD326	FALSE	TRUE	TRUE	TRUE	TRUE	FALSE	TRUE	TRUE	TRUE
	Marker	**HD#1**	**HD#2**	**HD#3**	**HD#4**	**HD#5**	**HD#6**	**HD#7**	**HD#8**	**HD#9**
#22	**CD14**	FALSE	FALSE	FALSE	TRUE	FALSE	FALSE	FALSE	FALSE	FALSE
	CD105	FALSE	FALSE	FALSE	FALSE	FALSE	FALSE	FALSE	FALSE	FALSE
	CD146	FALSE	FALSE	FALSE	FALSE	FALSE	FALSE	FALSE	FALSE	FALSE
	CD326	FALSE	FALSE	FALSE	TRUE	FALSE	FALSE	FALSE	FALSE	FALSE

methods and Table S4) in order to identify cancer-specific signatures and classify patients with cancer. We observed that, using the four markers which were highly enriched in breast cancer patients cited above, with a threshold of ≥ 3 positive markers to classify a sample as positive for cancer, we were able to reach a 78% sensitivity (7/9 patients detected) with a 100% specificity for the identification of breast cancer patients (Figure 4b, Table 1). Restricting the analysis to the more significantly different probes together with the threshold of ≥ 3 positive markers ensure a 100% specificity with no positivity detected for any healthy donors (Table S4).

Next, we analysed the EV surface protein levels normalized for each antibody-coated bead by the signal detected for the corresponding antibody isotype control (mIgG1 or recombinant antibody-REA). This normalization corrects for the background signal resulting from the total number of EVs in each sample (Figure 4c). For this analysis we had to exclude seven markers, including CD14, for which the corresponding control isotype (mIgG2a) was not provided in the commercial kit. We observed that CD326, CD146 and CD105 remained the three most significantly enriched markers ($P < 0.0001$) in breast cancer patients EVs compared to healthy donors. Indeed, these three markers displayed a stronger enrichment over their isotype control in breast cancer patients than in healthy donor samples (Figure 4d). These markers tended to be co-enriched in the same patients (see individual symbols in Figure S3b). We further integrated an arbitrary index consisting of the sum of the ratios of CD326, CD105 and CD146 MFI over their isotype, in order to compute a signal which could discriminate breast cancer patients from healthy donors (Figure 4e). We defined a threshold as follows: HD Index mean + 95% confidence interval (CI) = 28.86. This threshold discriminates eight breast cancer patients among the nine patients tested over healthy donors. The false negative P#24 was also not detected with the 'outlier' classifier described above. This patient was part of the low disease burden and non-progressive disease groups described previously and might have less tumour material in circulation. These results suggest that a small set of EV surface molecules could provide a disease signature and help identify patients with breast cancer.

4 | DISCUSSION

The work presented here highlights the value of different types of carriers circulating in plasma as sources of biomarkers in cancer: non-vesicular components for DNA and EVs for transmembrane proteins.

By systematic side-by-side comparison of different components of plasma, we demonstrated that, in metastatic breast cancer patients, separating EVs from smaller non-vesicular and/or soluble components does not improve the quality and sensitivity of detection of the nucleic acids analysed. Cellular DNA, both from total cells and from tumour origin, as well as mitochondrial DNA are as efficiently or more efficiently detected in total plasma. Circulating tumour DNA (ctDNA), for which we have previously demonstrated the predictive value when measuring its dynamic during the early phase of treatment (Darrigues et al., 2021; Jeannot et al., 2020), is detected in EV fraction but better recovered from total plasma at baseline and the non-vesicular extracellular forms are most prominently endowed with biomarker value. Our results confirm a recent study demonstrating that copy number variations (CNV) are detectable in DNA extracted from circulating EVs of breast cancer patient, but that standard ctDNA analysis has greater sensitivity for CNV detection and disease monitoring (Ruhen et al., 2020).

For mitochondrial DNA, which had been proposed by others as an EV-associated biomarker of relapse (Sansone et al., 2017), we confirmed here its higher abundance in plasma of breast cancer patients, although with no correlation with evolution of the disease. However, as opposed to Sansone et al., we observed its preferential association to EVs only in plasma from healthy donors, thus again, ruling out routine use of EV isolation for mtDNA biomarker analysis in patients. In patients, mtDNA is

also recovered in intermediate fractions of the SEC column, thus could be associated to smaller carriers than EVs. Such carriers could be exomeres/extracellular nanoparticles (Jeppesen et al., 2019; Zhang et al., 2018; Zhang et al., 2019): the subcellular origin of exomeres is completely unknown at the moment, whether they form in the lumen of multivesicular endosomes, in the secretory pathway, in the cytoplasm, or even in mitochondria has not yet been conclusively determined. Although this is not useful for a biomarker study, it would be interesting, for a basic science viewpoint, to determine the nature of the mtDNA-containing structures recovered in the EV-poor fractions of plasma. It is worth noting, however, that the plasma used here had been pre-processed following the standard-of-care method used for analysis of ctDNA, which includes a medium-speed centrifugation step (16,000 g, 10 min) to eliminate debris, apoptotic cells, but also some large EVs. It was recently shown that large EVs in plasma of prostate cancer patients and mouse models, contain more total DNA than small EVs, and contain tumour-associated DNA (Vagner et al., 2018). It would thus have been interesting, in our cohort, to quantify cfDNA and analyse MAF of ctDNA in the pellets obtained after the 16,000 g centrifugation, side by side with the total plasma: however, the routine process established to collect this cohort of samples at Institut Curie did not include recovery of this pellet. Future clinical trials should therefore consider keeping the platelet-poor medium-speed pellet, in addition to the post-medium speed plasma for exhaustive nucleic acid analyses. Finally, even though our work excludes EVs as a useful source of biomarker DNA, other nucleic acids such as RNA could still represent interesting EV-associated biomarkers: similar comparative studies of SEC fractions of plasma as we performed here should be implemented for the RNA cargo of EVs. Indeed, even if miRNA are the most commonly reported EV-associated biomarkers in the current literature, ongoing developments in the field suggest that miRNA are principally carried in blood by non-vesicular structures (Arroyo et al., 2011; Murillo et al., 2019), and this may be the case, or not, for many other types of RNAs that have been found in EVs, such as other small RNAs, long non-coding RNAs, etc.

The other important result of our study demonstrates that other components of EVs, analysed by a commercial kit, and thus amenable to routine clinical practice, potentially represent a valuable source of information in plasma of cancer patients: the set of three membrane-exposed proteins CD326/EPCAM, CD146/MCAM and CD105/ENG. We choose not to stress the potential use of CD14 as cancer marker, since we could not properly normalize the results for this molecule by the appropriate isotype control. CD14 is a monocyte-specific surface molecule, and unlikely to be expressed by tumour cells, thus its increased detection could illustrate alteration of the circulating immune system in the metastatic cancer patients, but this hypothesis would require further validation. EPCAM is expressed by normal epithelial cells, but also by carcinoma, and is often used to identify circulating tumour cells in cancer patients. In the multiplexed assay, it was not detected above background in healthy donor EVs, whereas it was clearly present in EVs of almost all patients, although the level was not high, suggesting that these EVs are relatively rare, thus probably originate from tumours. CD146 and CD105, by contrast, were already detected in EVs of healthy donors, which is consistent with their know expression by endothelial cells. The higher level of their detection on patient EVs could be linked to both altered vascular physiology, leading to the release of more EVs in the circulation, and, at least for CD146, to their possible expression on tumour-EVs. Indeed, the presence of CD146 was recently demonstrated on EVs from a mouse model of metastatic breast cancer (Ghoroghi et al., 2021). In addition to EPCAM, an already known marker of tumour EVs (Madhavan et al., 2014; Yang et al., 2017), our study identifies two novel candidate biomarkers for further exploration. We hope that our results will enable the design of a future routine clinical test for cancer patients, but these observations will first need to be validated in larger cohorts. Another advantage of the protein markers we have identified is their exposure on the surface of EVs, which could be exploited to enrich circulating EV preparations with tumour-derived EVs for further downstream analyses. Indeed, -omic studies of circulating EVs have recently been performed in cancer patients and/or mouse models, to identify protein signatures of cancer (Hoshino et al., 2020; Vinik et al., 2020). Large-range protein identification was achieved either by mass spectrometry (Hoshino et al., 2020), or by Reverse Phase Protein Array (Vinik et al., 2020). Both highlighted very few surface-exposed proteins, i.e., only an extracellular matrix protein, fibronectin, and the neural adhesion molecule N-cadherin in Vinik et al., or membrane proteins but expressed by non-tumoural cells, such as Immunoglobulins in Hoshino et al. Our observations are thus complementary, and also more amenable to routine implementation in a hospital configuration than would be systematic quantitative proteomic analyses of cancer patient samples.

Overall, our work paves the way for similar studies on other types of molecules for the identification of EV- or non-EV-associated biomarkers. We unravelled a shortlist of specific protein targets, which may provide strong added value in precision oncology. This needs follow-up clinical trials to demonstrate their detection at early stages of the disease or their differential expression in patients responding or not to chemo- or immuno-therapies.

ACKNOWLEDGEMENTS

We thank Drs. Joshua Welsh and Jennifer Jones, NCI, USA, for advice and feedback on MacsPlexExo analysis. This work was supported by Institut Curie, including through NCI.NIH-PIC3i-2018 program, INSERM, grants from INCa (11548), ANR (ANR-18-CE13-0017-03; ANR-18-CE15-0008-01; ANR-18-CE16-0022-02), Fondation ARC (PGA1 RF20180206962), French IdEx and LabEx DCBIOL (ANR-10-INSB-04, ANR-10-IDEX-0001-02 PSL, ANR-10-LABX-0038, ANR-11-LABX-0043 and ANR-18-IDEX-0001 Université de Paris).

AUTHOR CONTRIBUTIONS

Mercedes Tkach: Data curation; Formal analysis; Investigation; Methodology; Visualization; Writing—original draft; Writing—review & editing. **Caroline Hego:** Investigation; Methodology; Writing—original draft. **Marc Michel:** Formal analysis; Software. **Lauren Darrigues:** Data curation; Formal analysis. **Jean-Yves Pierga:** Resources. **François-Clément Bidard:** Resources. **Clotilde Théry:** Conceptualization; Data curation; Formal analysis; Funding acquisition; Methodology; Project administration; Resources; Supervision; Validation; Visualization; Writing—original draft; Writing—review & editing. **Charlotte Proudhon:** Conceptualization; Data curation; Formal analysis; Funding acquisition; Investigation; Methodology; Project administration; Resources; Supervision; Validation; Visualization; Writing—original draft; Writing—review & editing.

CONFLICT OF INTEREST

The authors have no disclosure.

ORCID

Mercedes Tkach https://orcid.org/0000-0002-8011-9444
Marc Michel https://orcid.org/0000-0001-6613-8027
Clotilde Théry https://orcid.org/0000-0001-8294-6884
Charlotte Proudhon https://orcid.org/0000-0002-4649-4574

REFERENCES

Arroyo, J. D., Chevillet, J. R., Kroh, E. M., Ruf, I. K., Pritchard, C. C., Gibson, D. F., Mitchell, P. S., Bennett, C. F., Pogosova-Agadjanyan, E. L., Stirewalt, D. L., Tait, J. F., & Tewari, M. (2011). Argonaute2 complexes carry a population of circulating microRNAs independent of vesicles in human plasma. *Proceedings of the National Academy of Sciences of the United States of America*, *108*, 5003–5008.

Chen, E., Cario, C. L., Leong, L., Lopez, K., Márquez, C. P., Chu, C., Li, P. S., Oropeza, E., Tenggara, I., Cowan, J., Simko, J. P., Chan, J. M., Friedlander, T., Wyatt, A. W., Aggarwal, R., Paris, P. L., Carroll, P. R., Feng, F., & Witte, J. S. (2021). Cell-free DNA concentration and fragment size as a biomarker for prostate cancer. *Scientific Reports-uk*, *11*, 5040.

Daly, R. -N., & O'Driscoll, L. (2021). Extracellular vesicles in blood: Are they viable as diagnostic and predictive tools in breast cancer? *Drug Discovery Today*, *26*, 778–785.

Darrigues, L., Pierga, J.-Y., Bernard-Tessier, A., Bià¨Che, I., Silveira, A. B., Michel, M., Loirat, D., Cottu, P., Cabel, L., Dubot, C., Geiss, R., Ricci, F., Vincent-Salomon, A., Proudhon, C., & Bidard, F.-C. (2021). Circulating tumor DNA as a dynamic biomarker of response to palbociclib and fulvestrant in metastatic breast cancer patients. *Breast Cancer Research*, *23*, 31. https://doi.org/10.1186/s13058-021-01411-0

Donovan, M. J., Noerholm, M., Bentink, S., Belzer, S., Skog, J., O'neill, V., Cochran, J. S., & Brown, G. A. (2015). A molecular signature of PCA3 and ERG exosomal RNA from non-DRE urine is predictive of initial prostate biopsy result. *Prostate Cancer and Prostatic Diseases*, *18*, 370–375.

Ghoroghi, S., Mary, B., Larnicol, A., Asokan, N., Klein, A., Osmani, N., Busnelli, I., Delalande, F., Paul, N., Halary, S., Gros, F., Fouillen, L., Haeberle, A.-M., Royer, C., Spiegelhalter, C., André-Grégoire, G., Mittelheisser, V., Detappe, A., Murphy, K., … Hyenne, V. (2021). Ral GTPases promote breast cancer metastasis by controlling biogenesis and organ targeting of exosomes. *Elife*, *10*, e61539.

Hoorn, E. J., Pisitkun, T., Zietse, R., Gross, P., Frokiaer, J., Wang, N. S., Gonzales, P. A., Star, R. A., & Knepper, M. A. (2005). Prospects for urinary proteomics: Exosomes as a source of urinary biomarkers. *Nephrology (Carlton, Vic.)*, *10*, 283–290.

Hoshino, A., Kim, H. S., Bojmar, L., Gyan, K. E., Cioffi, M., Hernandez, J., Zambirinis, C. P., Rodrigues, G., Molina, H., Heissel, S., Mark, M. T., Steiner, L., Benito-Martin, A., Lucotti, S., Di Giannatale, A., Offer, K., Nakajima, M., Williams, C., Nogués, L., … Lyden, D. (2020). Extracellular vesicle and particle biomarkers define multiple human cancers. *Cell*, *182*, 1044–1061.e18.

Jeannot, E., Darrigues, L., Michel, M., Stern, M. H., Pierga, J. Y., Rampanou, A., Melaabi, S., Benoist, C., Bièche, I., Vincent-Salomon, A., El Ayachy, R., Noret, A., Epaillard, N., Cabel, L., Bidard, F. C., & Proudhon, C. (2020). A single droplet digital PCR for ESR1 activating mutations detection in plasma. *Oncogene*, *39*, 1–9.

Jeppesen, D. K., Fenix, A. M., Franklin, J. L., Higginbotham, J. N., Zhang, Q., Zimmerman, L. J., Liebler, D. C., Ping, J., Liu, Q., Evans, R., Fissell, W. H., Patton, J. G., Rome, L. H., Burnette, D. T., & Coffey, R. J. (2019). Reassessment of exosome composition. *Cell*, *177*, 428–445.e18.

Jia, Y., Chen, Y., Wang, Q., Jayasinghe, U., Luo, X., Wei, Q., Wang, J., Xiong, H., Chen, C., Xu, B., Hu, W., Wang, L., Zhao, W., & Zhou, J. (2017). Exosome: Emerging biomarker in breast cancer. *Oncotarget*, *8*, 41717–41733.

Kahlert, C., Melo, S. A., Protopopov, A., Tang, J., Seth, S., Koch, M., Zhang, J., Weitz, J., Chin, L., Futreal, A., & Kalluri, R. (2014). Identification of double-stranded genomic DNA spanning all chromosomes with mutated KRAS and p53DNA in the serum exosomes of patients with pancreatic cancer. *Journal of Biological Chemistry*, *289*, 3869–3875.

Klump, J., Phillipp, U., Follo, M., Eremin, A., Lehmann, H., Nestel, S., Von Bubnoff, N., & Nazarenko, I. (2018). Extracellular vesicles or free circulating DNA: Where to search for BRAF and cKIT mutations? *Nanomedicine*, *14*, 875–882.

Koliha, N., Wiencek, Y., Heider, U., Jüngst, C., Kladt, N., Krauthã¤User, S., Johnston, I. C. D., Bosio, A., Schauss, A., & Wild, S. (2016). A novel multiplex bead-based platform highlights the diversity of extracellular vesicles. *Journal of Extracellular Vesicles*, *5*, 29975–29915.

Krug, A. K., Enderle, D., Karlovich, C., Priewasser, T., Bentink, S., Spiel, A., Brinkmann, K., Emenegger, J., Grimm, D. G., Castellanos-Rizaldos, E., Goldman, J. W., Sequist, L. V., Soria, J.-C., Camidge, D. R., Gadgeel, S. M., Wakelee, H. A., Raponi, M., Noerholm, M., & Skog, J. (2017). Improved EGFR mutation detection using combined exosomal RNA and circulating tumor DNA in NSCLC patient plasma. *Annals of Oncology*, *29*, 700–706.

Lázaro-Ibáñez, E., Sanz-Garcia, A., Visakorpi, T., Escobedo-Lucea, C., Siljander, P., Ayuso-Sacido, A., & Yliperttula, M. (2014). Different gDNA content in the subpopulations of prostate cancer extracellular vesicles: Apoptotic bodies, microvesicles, and exosomes. *Prostate*, *74*, 1379–1390.

Liao, Z., Jaular, L. M., Soueidi, E., Jouve, M., Muth, D. C., Schã¸Yen, T. H., Seale, T., Haughey, N. J., Ostrowski, M., Théry, C., & Witwer, K. W. (2019). Acetylcholinesterase is not a generic marker of extracellular vesicles. *Journal of Extracellular Vesicles*, *8*, 1628592.

Lowry, M. C., Gallagher, W. M., & O'driscoll, L. (2015). The role of exosomes in breast cancer. *Clinical Chemistry*, *61*, 1457–1465.

Madhavan, B., Yue, S., Galli, U., Rana, S., Gross, W., Müller, M., Giese, N. A., Kalthoff, H., Becker, T., Büchler, M. W., & Zöller, M. (2014). Combined evaluation of a panel of protein and miRNA serum-exosome biomarkers for pancreatic cancer diagnosis increases sensitivity and specificity. *International Journal of Cancer*, *136*, 2616–2627.

Matsuzaki, J., & Ochiya, T. (2017). Circulating microRNAs and extracellular vesicles as potential cancer biomarkers: A systematic review. *International Journal of Clinical Oncology*, *22*, 413–420.

Melo, S. A., Luecke, L. B., Kahlert, C., Fernandez, A. F., Gammon, S. T., Kaye, J., Lebleu, V. S., Mittendorf, E. A., Weitz, J., Rahbari, N., Reissfelder, C., Pilarsky, C., Fraga, M. F., Piwnica-Worms, D., & Kalluri, R. (2015). Glypican-1 identifies cancer exosomes and detects early pancreatic cancer. *Nature*, *523*, 177–182.

Murillo, O. D., Thistlethwaite, W., Rozowsky, J., Subramanian, S. L., Lucero, R., Shah, N., Jackson, A. R., Srinivasan, S., Chung, A., Laurent, C. D., Kitchen, R. R., Galeev, T., Warrell, J., Diao, J. A., Welsh, J. A., Hanspers, K., Riutta, A., Burgstaller-Muehlbacher, S., Shah, R. V., … Milosavljevic, A. (2019). exRNA atlas analysis reveals distinct extracellular RNA cargo types and their carriers present across human biofluids. *Cell*, *177*, 463–477.e15.

Nanou, A., Coumans, F. A. W., Van Dalum, G., Zeune, L. L., Dolling, D., Onstenk, W., Crespo, M., Fontes, M. S., Rescigno, P., Fowler, G., Flohr, P., Brune, C., Sleijfer, S., De Bono, J. S., & Terstappen, L. W. M. M. (2018). Circulating tumor cells, tumor-derived extracellular vesicles and plasma cytokeratins in castration-resistant prostate cancer patients. *Oncotarget*, *9*, 19283–19293.

Nanou, A., Miller, M. C., Zeune, L. L., De Wit, S., Punt, C. J. A., Groen, H. J. M., Hayes, D. F., De Bono, J. S., & Terstappen, L. W. M. M. (2020). Tumour-derived extracellular vesicles in blood of metastatic cancer patients associate with overall survival. *British Journal of Cancer*, *122*, 801–811.

Nanou, A., Zeune, L. L., Bidard, F.-C., Pierga, J.-Y., & Terstappen, L. W. M. M. (2020). HER2 expression on tumor-derived extracellular vesicles and circulating tumor cells in metastatic breast cancer. *Breast Cancer Research*, *22*, 86.

Riva, F., Bidard, F.-C., Houy, A., Saliou, A., Madic, J., Rampanou, A., Hego, C., Milder, M., Cottu, P., Sablin, M.-P., Vincent-Salomon, A., Lantz, O., Stern, M.-H., Proudhon, C., & Pierga, J.-Y. (2017). Patient-specific circulating tumor DNA detection during neoadjuvant chemotherapy in triple-negative breast cancer. *Clinical Chemistry*, *63*, 691–699. https://doi.org/10.1373/clinchem.2016.262337

Ruhen, O., Mirzai, B., Clark, M. E., Nguyen, B., Salomon, C., Erber, W., & Meehan, K. (2020). Comparison of circulating tumour DNA and extracellular vesicle DNA by low-pass whole-genome sequencing reveals molecular drivers of disease in a breast cancer patient. *Biomedicines*, *9*, 14.

Sansone, P., Savini, C., Kurelac, I., Chang, Q., Amato, L. B., Strillacci, A., Stepanova, A., Iommarini, L., Mastroleo, C., Daly, L., Galkin, A., Thakur, B. K., Soplop, N., Uryu, K., Hoshino, A., Norton, L., Bonafé, M., Cricca, M., Gasparre, G., … Bromberg, J. (2017). Packaging and transfer of mitochondrial DNA via exosomes regulate escape from dormancy in hormonal therapy-resistant breast cancer. *Proceedings of the National Academy of Sciences of the United States,of America*, *114*, E9066–E9075.

Skog, J., Würdinger, T., Van Rijn, S., Meijer, D. H., Gainche, L., Curry, W. T., Carter, B. S., Krichevsky, A. M., & Breakefield, X. O. (2008). Glioblastoma microvesicles transport RNA and proteins that promote tumour growth and provide diagnostic biomarkers. *Nature Cell Biology*, *10*, 1470–1476.

Stroun, M., Anker, P., Lyautey, J., Lederrey, C., & Maurice, P. A. (1987). Isolation and characterization of DNA from the plasma of cancer patients. *European Journal of Cancer & Clinical Oncology*, *23*, 707–712.

Thakur, B. K., Zhang, H., Becker, A., Matei, I., Huang, Y., Costa-Silva, B., Zheng, Y., Hoshino, A., Brazier, H., Xiang, J., Williams, C., Rodriguez-Barrueco, R., Silva, J. M., Zhang, W., Hearn, S., Elemento, O., Paknejad, N., Manova-Todorova, K., Welte, K., … Lyden, D. (2014). Double-stranded DNA in exosomes: A novel biomarker in cancer detection. *Cell Research*, *24*, 766–769.

Thakur, K., Singh, M. S., Feldstein-Davydova, S., Hannes, V., Hershkovitz, D., & Tsuriel, S. (2021). Extracellular vesicle-derived DNA vs. CfDNA as a biomarker for the detection of colon cancer. *Genes*, *12*, 1171.

Vagner, T., Spinelli, C., Minciacchi, V. R., Balaj, L., Zandian, M., Conley, A., Zijlstra, A., Freeman, M. R., Demichelis, F., De, S., Posadas, E. M., Tanaka, H., & Di Vizio, D. (2018). Large extracellular vesicles carry most of the tumour DNA circulating in prostate cancer patient plasma. *Journal of Extracellular Vesicles*, *7*, 1505403.

van der Loo, M. P. J. (2010).Distribution based outlier detection with the extremevalues package. User at <http://www.markvanderloo.eu/files/statistics/useR2010_van_der_Loo.pdf>

Vinik, Y., Ortega, F. G., Mills, G. B., Lu, Y., Jurkowicz, M., Halperin, S., Aharoni, M., Gutman, M., & Lev, S. (2020). Proteomic analysis of circulating extracellular vesicles identifies potential markers of breast cancer progression, recurrence, and response. *Science Advances*, *6*, eaba5714.

Yang, K. S., Im, H., Hong, S., Pergolini, I., Del Castillo, A. F., Wang, R., Clardy, S., Huang, C.-H., Pille, C., Ferrone, S., Yang, R., Castro, C. M., Lee, H., Del Castillo, C. F., & Weissleder, R. (2017). Multiparametric plasma EV profiling facilitates diagnosis of pancreatic malignancy. *Science Translational Medicine*, *9*, eaal3226.

Zhang, H., Freitas, D., Kim, H. S., Fabijanic, K., Li, Z., Chen, H., Mark, M. T., Molina, H., Martin, A. B., Bojmar, L., Fang, J., Rampersaud, S., Hoshino, A., Matei, I., Kenific, C. M., Nakajima, M., Mutvei, A. P., Sansone, P., Buehring, W., … Lyden, D. (2018). Identification of distinct nanoparticles and subsets of extracellular vesicles by asymmetric flow field-flow fractionation. *Nature Cell Biology*, *20*, 332–343. https://doi.org/10.1038/s41556-018-0040-4

Zhang, Q., Higginbotham, J. N., Jeppesen, D. K., Yang, Y.-P., Li, W., Mckinley, E. T., Graves-Deal, R., Ping, J., Britain, C. M., Dorsett, K. A., Hartman, C. L., Ford, D. A., Allen, R. M., Vickers, K. C., Liu, Q., Franklin, J. L., Bellis, S. L., & Coffey, R. J. (2019). Transfer of functional cargo in exomeres. *Cell Reports*, *27*, 940–954.e6.

SUPPORTING INFORMATION

Additional supporting information can be found online in the Supporting Information section at the end of this article.

How to cite this article: Tkach, M., Hego, C., Michel, M., Darrigues, L., Pierga, J.-Y., Bidard, F.-C., Théry, C., & Proudhon, C. (2022). Circulating extracellular vesicles provide valuable protein, but not DNA, biomarkers in metastatic breast cancer. *Journal of Extracellular Biology*, *1,* e51. https://doi.org/10.1002/jex2.51